


## Dust charging and levitating in a sheath of plasma containing energetic particles

Jing Ou(欧靖), Xiao-Yun Zhao(赵晓云), Bin-Bin Lin(林滨滨)
**Citation:**Chin. Phys. B . 2018, 27(2): 025204. **doi:** 10.1088/1674-1056/27/2/025204

Journal homepage: http://cpb.iphy.ac.cn; http://iopscience.iop.org/cpb

**What follows is a list of articles you may be interested in**

---

### Sheath structure in plasma with two species of positive ions and secondary electrons

Xiao-Yun Zhao(赵晓云), Nong Xiang(项农), Jing Ou(欧靖), De-Hui Li(李德徽), Bin-Bin Lin(林滨滨)
Chin. Phys. B . 2016, 25(2): 025202. **doi:** 10.1088/1674-1056/25/2/025202

### Effects of *q*-profiles of a weak magnetic shear on energetic ion excited *q*=1 mode in tokamak plasmas

Ze-Yu Li(李泽宇), Xian-Qu Wang(王先驱), Xiao-Gang Wang(王晓钢)
Chin. Phys. B . 2016, 25(1): 015203. **doi:** 10.1088/1674-1056/25/1/015203

### A two-dimensional model of He/$O_2$ atmospheric pressure plasma needle discharge

Qian Mu-Yang, Yang Cong-Ying, Chen Xiao-Chang, Liu San-Qiu, Yan Wen, Liu Fu-Cheng, Wang De-Zhen
Chin. Phys. B . 2015, 24(12): 125203. **doi:** 10.1088/1674-1056/24/12/125203

### Effects of some parameters on the divertor plasma sheath characteristics and fuel retention in castellated tungsten tile gaps

Sang Chao-Feng, Dai Shu-Yu, Sun Ji-Zhong, Bonnin Xavier, Xu Qian, Ding Fang, Wang De-Zhen
Chin. Phys. B . 2014, 23(11): 115201. **doi:** 10.1088/1674-1056/23/11/115201

### Characteristics of wall sheath and secondary electron emission under different electron temperatures in a Hall thruster

Duan Ping, Qin Hai-Juan, Zhou Xin-Wei, Cao An-Ning, Chen Long, Gao Hong
Chin. Phys. B . 2014, 23(7): 075203. **doi:** 10.1088/1674-1056/23/7/075203

---

# Dust charging and levitating in a sheath of plasma containing energetic particles*

Jing Ou(欧靖)[1,2,†], Xiao-Yun Zhao(赵晓云)[1,3], and Bin-Bin Lin(林滨滨)[1]

[1] *Institute of Plasma Physics, Chinese Academy of Sciences, Hefei* 230031, *China*
[2] *Magnetic Fusion Theory, Chinese Academy of Sciences, Hefei* 230031, *China*
[3] *School of Physics and Electronic Engineering, Fuyang Normal University, Fuyang* 236037, *China*

(Received 18 October 2017; revised manuscript received 20 November 2017; published online 5 January 2018)

The structure of the sheath in the presence of energetic particles is investigated in the multi-fluid framework. Based on the orbital motion limited (OML) theory, the dust grain charging inside the sheath of plasma containing energetic particles is examined for the carbon wall, and then the effect of the energetic particles on the stationary dust particle inside the sheath is discussed through the trapping potential energy. It is found that with the increase of energetic ion concentration or energy, the size of dust staying in levitation equilibrium decreases and the levitating position is much closer to the wall. In the case of deuterium ions as energetic ions, the bigger dust particle can be trapped by the sheath than in the case of hydrogen ions as energetic ions. When the energetic electron component is present, the levitating position of dust particle in the sheath depends strongly on the energetic electron. The levitating dust particle is closer to the wall as the energetic electron energy or concentration is increased. In addition, with the increase of temperature of thermal background ion, the size of dust particle trapped by the sheath decreases and the levitating positions of dust particles with the same size radius inside the sheath move toward the wall. Our results can be helpful in investigating the property of the sheath where the energetic particle component is present.

**Keywords:** sheath, energetic particles, dust particle

**PACS:** 52.40.Kh, 52.27.Lw, 52.30.Ex **DOI:** 10.1088/1674-1056/27/2/025204

## 1. Introduction

The dust particle is an important and serious problem in a large variety of plasma applications including plasma processing and fusion research. These particles mainly result from plasma surface interaction process. The plasma-surface interaction may become strong when an energetic particle component is present. For instance, in tokamak discharge, during radiofrequency wave heating or neutral beam injection (NBI), the energetic particles appear in the device edge region.[1–5] It is found that hot spots would be a main source for the dust production during long pulse discharge with lower hybrid current drive (LHCD),[6] and dust rate increases with increasing the power of NBI.[7] As is well known, the presence of energetic particles can change the sheath structure.[8–13] A natural question is whether energetic particles can influence dust particles in the sheath. Combining with other diagnostic tools such as laser scattering and fast cameras, the investigation of the dust particles inside the sheath is a way to study the lifetime of the wall material because a lot of dust particles imply the strong plasma-wall interaction.[14]

On the other hand, the presence of a dust particle inside the sheath can provide a useful guide in measuring the sheath characteristics.[15–18] By using fine dust probes, sheath characteristics can be investigated in considerable detail, though indirectly, due to the fact that the charge on the dust particle depends on the local plasma condition. The dynamics of a dust particle in such a surrounding can provide information about the electron and ion fluxes, and also about the sheath potential and electric field. The present investigation is motivated by such a goal for the sheath of plasma containing energetic particles and thus, will be undertaken in a study of the dust behavior in the levitated equilibrium inside the sheath after ascertaining the comparative role of energetic particles in the sheath characteristics.

The dust particle in a plasma sheath has become a topic of many studies in fusion, astrophysical and laboratory plasmas. Dust particles in the sheath can be considered to be isolated if the dust components are sparse.[14,15,19,20] However, they can modify the structure of the plasma-sheath region if its density is relatively high.[17,18,21,22] In the case where the energetic electrons exist in the sheath, both an isolated grain and a dense cloud of dust particles in a sheath with plasma wall bias have been studied.[17,18,20] In a floating sheath, the wall potential is determined by the zero total current at the wall, and it depends strongly on the energetic electron and the secondary electron emission (SEE). Furthermore, it can

*Project supported by the National Natural Science Foundation of China (Grant No. 11475223), the National Magnetic Confinement Fusion Science Program of China (Grant No. 2015GB101003), and the JSPS-NRF-NSFC A3 Foresight Program in the field of Plasma Physics (Grant Nos. 11261140328 and 2012K2A2A6000443).

†Corresponding author. E-mail: ouj@ipp.ac.cn

© 2018 Chinese Physical Society and IOP Publishing Ltd 

demonstrate a sharp transition at a certain energetic electron flux.[8–11] In addition, most of the researches mentioned above have been carried out on the assumption that ion temperature is far lower than electron temperature so that the effects of the ion directional velocity on the dust charging and dynamics are omitted.[15,17–20] In some plasmas such as fusion plasma, ion temperature is usually comparable to or even higher than electron temperature and their directional velocity may be very large if the sheath of plasma contains energetic ions. As a result, the charging of the dust particle depends on the ion directional velocity.[23]

In order to investigate the dust particle in an electrostatic sheath of plasma containing energetic ions or energetic electrons, we focus on the effects of the energetic particles on the dust charging and levitation for carbon (C) wall. In addition, we also discuss the variations of the dust charging and levitation for the different temperatures of thermal background ion. The rest of this paper is organized as follows. In Section 2, the sheath model based on one-dimensional (1D) multi-fluid equations is described for the carbon wall, and the effect of the energetic particles on the sheath structure is presented. In Section 3, the dust charging model and levitation equilibrium in the sheath are discussed for various concentrations and energies of energetic particles. General conclusions are drawn in Section 4.

## 2. Sheath of plasma containing energetic particles

### 2.1. Sheath model

To investigate the levitating dust particles in a steady-state sheath of plasma containing energetic particles, we present a 1D, multi-fluid unmagnetized electrostatic sheath model, whose constituents are thermal background electrons and single charge ions, the energetic particles including ions or electrons, and the emitted electrons from the wall. In the model, the impurity sputtering from the wall surface and collision are not taken into account. Moreover, we assume that the impurity density is much lower than that of background ions and thus the impurity does not disturb the plasma.[14,24,25] The dust particle is assumed to be isolated and then cannot modify the sheath. For the thermal background and energetic ions, the continuity and momentum equations are

$$\frac{\mathrm{d}}{\mathrm{d}z}(n_{\mathrm{i},j}v_{\mathrm{i},j}) = 0, \tag{1}$$

$$m_{\mathrm{i},j}v_{\mathrm{i},j}\frac{\mathrm{d}v_{\mathrm{i},j}}{\mathrm{d}z} = -e\frac{\mathrm{d}\varphi}{\mathrm{d}z} - \frac{1}{n_{\mathrm{i},j}}\frac{\mathrm{d}p_{\mathrm{i},j}}{\mathrm{d}z}, \tag{2}$$

where $z$ is the distance from the sheath edge with the plasma-sheath boundary located at $z = 0$, $\varphi$ and $e$ are the electrostatic potential and electron charge, respectively, $m_{\mathrm{i},j}$ is the ion mass, $n_{\mathrm{i},j}$ is the ion number density, $v_{\mathrm{i},j}$ is the ion fluid velocity, and $p_{\mathrm{i},j}$ is the ion pressure of background ions and energetic ions with $j = 1, 2$ and is expressed as $p_{\mathrm{i},j} = \gamma_j k_{\mathrm{B}} T_{\mathrm{i},j} n_{\mathrm{i},j}$ with $k_{\mathrm{B}}$ being the Boltzmann constant, $T_{\mathrm{i},j}$ the ion temperature, and $\gamma$ the polytropic coefficient. Here, isothermal approximation $\gamma = 1$ is used.

The electrons from the bulk plasma region far away from the sheath are assumed to be Maxwellian. After they enter into the sheath, their 1D velocity distribution function approaching the wall can be described by a truncated Maxwellian distribution function,

$$f_{\mathrm{e},j}(u_{\mathrm{e},j}) = \begin{cases} \dfrac{n_{\mathrm{e},j}(0)}{\sqrt{2\pi}I_{\mathrm{e},j}u_{t\mathrm{e},j}} \exp\left(-\dfrac{u_{\mathrm{e},j}^2}{2u_{t\mathrm{e},j}^2}\right), & u_{ce,j} < u_{\mathrm{e},j} < \infty, \\ 0, & \text{otherwise.} \end{cases} \tag{3}$$

Here, subscripts e, $j$ = e, 1 and e, $j$ = e, 2 denote the thermal background electron and energetic electron, respectively, $n_{\mathrm{e},j}$ is the electron number density, $u_{t\mathrm{e},j} = \sqrt{k_{\mathrm{B}}T_{\mathrm{e},j}/m_{\mathrm{e}}}$ is the electron thermal velocity with electron temperature $T_{\mathrm{e},j}$ and electron mass $m_{\mathrm{e}}$, $u_{ce,j}$ is cutoff velocity with $u_{ce,j} > -\sqrt{2ek_{\mathrm{B}}T_{\mathrm{e},j}(\varphi_w - \varphi)/m_{\mathrm{e}}}$ and this cutoff velocity yields the electron normalization coefficient $I_{\mathrm{e},j} = [1 + \mathrm{erf}(\sqrt{e\varphi_w/(k_{\mathrm{B}}T_{\mathrm{e},j})})]/2$. The subscript $w$ denotes the sheath-wall boundary located at $z = w$. Based on Eq. (3), the profile of the electron density in the sheath and electron flux to the wall can be written respectively as

$$n_{\mathrm{e},j} = n_{\mathrm{e},j}(0)\exp[-e\varphi/(k_{\mathrm{B}}T_{\mathrm{e},j})] \times \frac{1+\mathrm{erf}[\sqrt{e(\varphi_w-\varphi)/(k_{\mathrm{B}}T_{\mathrm{e},j})}]}{1+\mathrm{erf}[\sqrt{e\varphi_w/(k_{\mathrm{B}}T_{\mathrm{e},j})}]}, \tag{4}$$

$$\Gamma_{\mathrm{e},j} = n_{\mathrm{e},j}(0)\exp[-e\varphi_w/(k_{\mathrm{B}}T_{\mathrm{e},j})]\frac{1}{I_{\mathrm{e},j}}\sqrt{\frac{k_{\mathrm{B}}T_{\mathrm{e},j}}{2\pi m_{\mathrm{e}}}}. \tag{5}$$

On the assumption that the secondary emission at the material surface has a negligible speed, the energy balance and flux conservation equations in the sheath can be written as

$$\frac{1}{2}m_{\mathrm{e}}v_{\mathrm{es}}^2 = e(\varphi_w - \varphi), \tag{6}$$

$$n_{\mathrm{es}}V_{\mathrm{es}} = \Gamma_{\mathrm{es}}. \tag{7}$$

Here, $\Gamma_{\mathrm{es}} = \Gamma_{\mathrm{es},1} + \Gamma_{\mathrm{es},2}$ is the flux of the secondary emission electron including $\Gamma_{\mathrm{es},1}$ caused by background electrons and $\Gamma_{\mathrm{es},2}$ caused by the energetic electrons. We assume that SEE due to ion impact is negligible because it is not important unless ion impact energies are greater than 1Kev while the electron induced SEE is significant even at rather modest energies greater than 30 eV.[26] With SEE coefficient $\delta_{\mathrm{e},j}$, $\Gamma_{\mathrm{es},j}$ can be expressed as

$$\Gamma_{\mathrm{es},j} = \Gamma_{\mathrm{e},j}\frac{1}{n_{\mathrm{e},j}(0)}\int_0^\infty f_{\mathrm{e},j}(E_{\mathrm{p}} - e\varphi_w)\delta_{\mathrm{e},j}(E_{\mathrm{p}})\,\mathrm{d}E_{\mathrm{p}}. \tag{8}$$

Here, $E_{\rm p}$ is the kinetic energy of the incident electron. We use the Young–Dekker formula[27]

$$\delta(E_{\rm p}) = \frac{\delta_{\rm m}}{1-\exp(-x_{\rm m})}\left(\frac{E_{\rm p}}{E_{\rm m}}\right)^{1-k} \times \left\{1-\exp\left[-x_{\rm m}\left(\frac{E_{\rm p}}{E_{\rm m}}\right)^{k}\right]\right\},$$

in which $x_{\rm m}=[1-(1/k)][\exp(x_{\rm m}-1)]$, $\delta_{\rm m}$ is the maximum of $\delta$, and $E_{\rm m}$ is the characteristic energy corresponding to $\delta_{\rm m}$. For the carbon, $\delta_{\rm m}=0.708$ and $E_{\rm m}=350$ eV.[28]

Then, a profile of secondary electron density is

$$n_{\rm es}=\Gamma_{\rm es}/\sqrt{\frac{2e(\varphi_w-\varphi)}{m_{\rm e}}}. \tag{9}$$

The sheath system of equations is closed by the Poisson equation

$$\frac{{\rm d}^2\varphi}{{\rm d}z^2}=-\frac{e}{\varepsilon_0}(n_{{\rm i},j}-n_{{\rm e},j}-n_{\rm es}), \tag{10}$$

where, $\varepsilon_0$ is the permittivity of the free space. The Poisson's equation boundary conditions are given as follows: at the wall the floating potential $\varphi_w$ is determined from the balance between electron flux and ion flux, i.e.,

$$n_{{\rm i},j}(0)v_{{\rm i}0,j}=\Gamma_{{\rm e},j}-\Gamma_{\rm es}; \tag{11}$$

at the sheath edge$z=0$, the electric potential is taken to be zero, where the electric field is assumed to be very small, i.e.,

$$\phi=0,\ \ |{\rm d}\phi/{\rm d}x|<<1, \tag{12}$$

and the quasi-neutrallity condition is satisfied

$$n_{{\rm i},j}(0)=n_{{\rm e},j}(0)+n_{\rm es}(0). \tag{13}$$

For the multi-ion-component plasma collisionless sheath, it is suggested from both analytical and numerical results that each ion species should satisfy its own Bohm criterion at the sheath edge.[13,29,30] When there are more than the population of negatively charged particles in the plasma sheath, by following Riemann,[31] the Bohm criterion can be written as

$$v_{{\rm i}0,j}\geq C_{{\rm s},j}=\sqrt{(T_{\rm scr}+\gamma_j T_{{\rm i},j})/m_{{\rm i},j}}, \tag{14}$$

where $T_{\rm scr}$ is the electron screening temperature, defined as $T_{\rm scr}=en_{\rm e}(\varphi)/{\rm d}n_{\rm e}/{\rm d}\varphi|_{\varphi=0}$ in which $n_{\rm e}(\varphi)$ can be obtained from the electron density distributions Eqs. (4) and (8) including thermal background electrons, energetic electrons and secondary emission electrons. In the following discussion, we only consider $v_{\rm i0}=C_{\rm s}$, i.e., Bohm criterion in a marginal form.

Next, we normalize Eqs. (1), (2), (4), (9), and (10) with the following set of dimensionless variables

$$\phi=-\frac{e\varphi}{k_{\rm B}T_{\rm e,1}},\ \ \xi=\frac{z}{\lambda_{\rm De}},\ \ u_{{\rm i},j}=\frac{v_{{\rm i},j}}{c_{\rm i}},\ \ N_{{\rm i},j}=\frac{n_{{\rm i},j}}{n_{{\rm i},j}(0)},$$

$$N_{{\rm e},j}=\frac{n_{{\rm e},j}}{n_{{\rm e},j}(0)},\ \ N_{\rm es}=\frac{n_{\rm es}}{n_{{\rm e},s}(0)},\ \ \mu=\frac{m_{{\rm i},j}}{m_{\rm i,1}},\ \ \alpha_{\rm i}=\frac{n_{i,2}(0)}{n_{\rm i,1}},$$

$$\alpha_{\rm e}=\frac{n_{\rm e,2}(0)}{n_{\rm e,1}},\ \ \beta_{{\rm i},j}=\frac{T_{{\rm i},j}}{T_{\rm i,1}},\ \ \beta_{{\rm e},j}=\frac{T_{{\rm e},j}}{T_{\rm e,1}},\ \ \beta_{\rm T}=\frac{T_{\rm i,1}}{T_{\rm e,1}}, \tag{15}$$

where $\lambda_{\rm De}=\sqrt{\varepsilon_0 T_{\rm e,1}/[e^2 n_{\rm e,1}(0)]}$ is the electron Debye length. The parameter $c_{\rm i}=\sqrt{k_{\rm B}T_{\rm e,1}/m_{\rm i,1}}$ is the velocity on a normalized reference scale. At the sheath edge, according to Eqs. (5) and (9), the density ratio of secondary emission electron to thermal electron is

$$\alpha_{{\rm e},s}=\frac{\delta_{\rm e,1}\exp(\phi_w)/I_{\rm e1}+\delta_{\rm e,2}\alpha_{\rm e}\exp(\phi_w/\beta_{\rm e,2})\sqrt{\beta_{\rm e,2}}/I_{\rm e2}}{2\sqrt{-\pi\phi_w}}$$

and the density ratio of ions to thermal electron satisfy $\alpha_{\rm T}=[(1+\alpha_{\rm e})+\alpha_{{\rm e},s}]/(1+\alpha_{\rm i})$ under the quasi-neutrality condition [Eq. (13)]. The $\varphi_w$ will be obtained under the current balance condition [Eq. (11)]. By using the above normalization, the following set of coupled equations can be obtained:

$$\frac{{\rm d}N_{{\rm i},j}}{{\rm d}\xi}=\frac{N_{{\rm i},j}}{\mu(u_{{\rm i},j}^2-\gamma_j N_{{\rm i},j}^{\gamma_j-1}\beta_{{\rm i},j}\beta_{\rm T})}\frac{{\rm d}\phi}{{\rm d}\xi}, \tag{16}$$

$$\frac{{\rm d}u_{{\rm i},j}}{{\rm d}\xi}=-\frac{u_{{\rm i},j}}{\mu(u_{{\rm i},j}^2-\gamma_j N_{{\rm i},j}^{\gamma_j-1}\beta_{{\rm i},j}\beta_{\rm T})}\frac{{\rm d}\phi}{{\rm d}\xi}, \tag{17}$$

$$N_{{\rm e},j}=N_{{\rm e},j}(0)\exp(\phi/\beta_{{\rm e},j})\frac{1+{\rm erf}(\sqrt{(\phi-\phi_w)/\beta_{{\rm e},j}})}{1+{\rm erf}(\sqrt{-\phi_w/\beta_{{\rm e},j}})}, \tag{18}$$

$$N_{{\rm e},s}=\frac{\delta_{\rm e,1}\exp(\phi_w)/I_{\rm e1}+\alpha_{\rm e}\delta_{\rm e,2}\exp(\phi_w/\beta_{\rm e,2})\sqrt{\beta_{\rm e,2}}/I_{\rm e2}}{2\sqrt{\pi\phi-\phi_w}}, \tag{19}$$

$$\frac{{\rm d}^2\phi}{{\rm d}\xi^2}=\alpha_{\rm T}N_{\rm i,1}+\alpha_{\rm T}\alpha_{\rm i}N_{i,2}-N_{\rm e,1}-\alpha_{\rm e}N_{\rm e,2}-\alpha_{\rm es}N_{{\rm e},s}. \tag{20}$$

To solve Eqs. (16)–(20), the fourth-order Runge–Kutta method is used under the appropriate boundary conditions at the plasma-sheath edge. Starting from $\xi=0$, we proceed in space until the sheath potential $\phi=\phi_w$. In this process, the normalized sheath length thickness $D$ is determined and the distance from the wall to any point in the sheath $x=D-\xi$ can be obtained. In all the results reported in this paper, C is considered as the wall material and deuterium is considered to be the background gas by adopting $n_{\rm e,1}(0)=10^{17}$ m$^{-3}$ and $T_{\rm e,1}=10$ eV, which are in the range of parameters of the EAST tokamak near the low hybrid wave antenna. The energetic ion component is considered to be the deuterium ion due to NBI or the hydrogen ion due to ion cyclotron resonance heating (ICRH). The deuterium ion is used as default energetic ion and $T_{\rm e,1}=T_{\rm i,1}$ unless otherwise stated.

### 2.2. Sheath results

For a collisionless sheath, the floating potential can be obtained directly from the current balance condition. When the energetic ion component is present, an estimate of the energetic ions affecting significantly on the sheath indicates that their concentration $\alpha_{\rm i}$ is greater than $\sqrt{T_{\rm e,1}/(\gamma T_{i,2})}$.[13] Under the same parameters, due to the smaller mass and the resulting

larger energetic ion flux, the potential drop across the sheath in the case of the hydrogen ion as an energetic ion component is smaller than in the case of the deuterium ion as the energetic ion component. When the energetic electron component is present in the sheath as shown in Fig. 1(a), the sheath potential can show a very large drop even with a small fraction.[8–11] Once the sheath potential presents a sharp transition, the energetic electron begins to dominate the sheath, which indicates that the ion energy flux toward the wall becomes very large and then plasma-wall interaction may become serious. According to the current balance condition, the sheath potential varies as the temperature of background ion is changed. This is the case appearing in the fusion plasma, in which the background ion temperature may be higher than the background electron temperature during the NBI or ICRH, while it may be lower than the background electron temperature during the LHCD. Figure 1(b) shows the dependence of the sheath potential on the temperature of background ions and the concentration of energetic electrons.

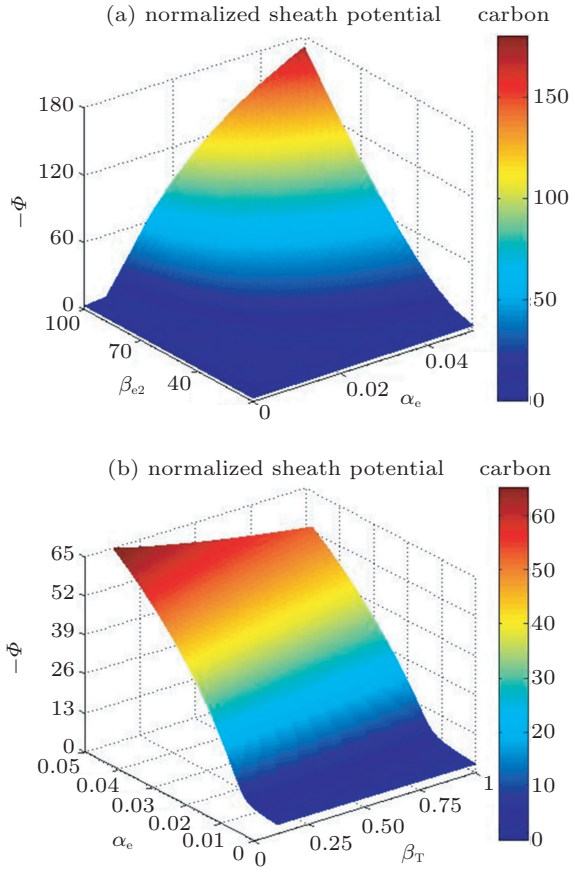



**Fig. 1.** (color online) Normalized sheath potentials, respectively, as a function of (a) energetic electron concentration and energy and (b) energetic electron concentration and temperature of background ions with $\beta_{e,2} = 50$.

With the given values of $\alpha_i$, $\alpha_e$, $\beta_{i,j}$, $\beta_{e,j}$, and $\beta_T$, after obtaining the sheath floating potential, we can calculate the sheath boundary conditions at the sheath edge including the background and energetic ion velocity and background ion density, and then obtain the profiles of sheath potential and plasma parameters inside the sheath based on Eqs. (16)–(20).

Figures 2 and 3 show the profiles of the sheath potential, background electron and ion density, and energetic particle density in the sheath. By comparing the effects of the hydrogen ion and deuterium ion serving as the energetic ion components on the sheath, we can find in Fig. 2 that the profiles of the sheath potential, and thermal background ion and electron densities almost have no difference among each other, except energetic ion density. Figure 3 shows that the sheath structure depends strongly on energetic electrons. Even a small fraction of energetic electrons can lead to a large difference in profile between the sheath potential and the plasma parameters.

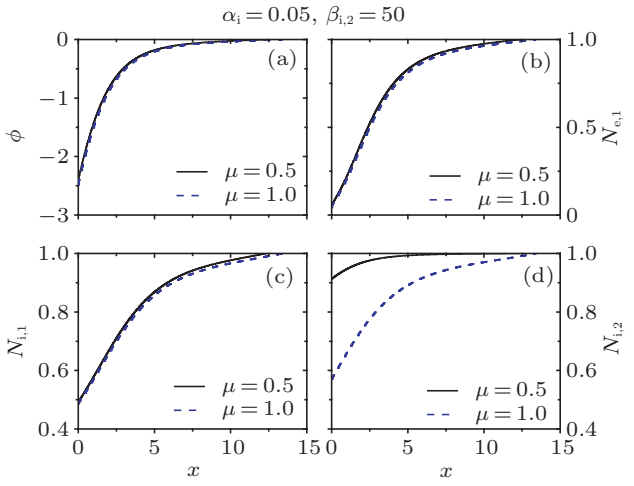



**Fig. 2.** Profiles of the normalized sheath potentials, background electron and ion densities, and energetic particle densities in the sheaths as a function of distance from the plasma sheath to the wall.

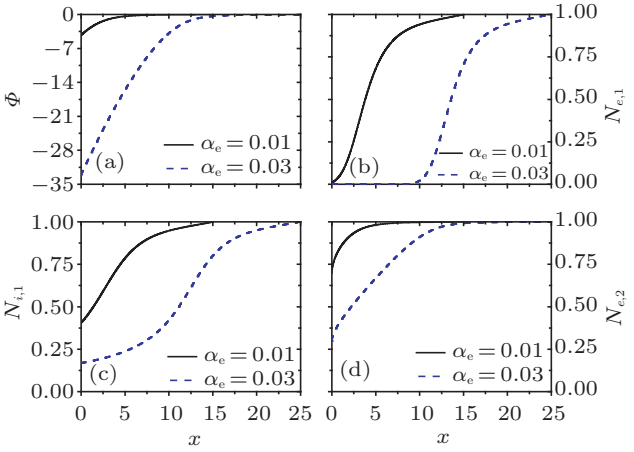



**Fig. 3.** Profiles of the normalized sheath potentials, background electron and ion densities, and energetic particle densities in the sheaths as a function of distance from the plasma sheath to the wall for $\beta_{e,2} = 50$.

To investigate the effect of the background ion temperature on the sheath of plasma containing energetic ions or energetic electrons, we plot and compare the profiles of the sheath potential, background electron and ion density, and energetic particle density in the sheath in Fig. 4. For the high temperature of background ion, sheath potential is smaller while the plasma parameters are larger when the energetic ion or electron component is present.

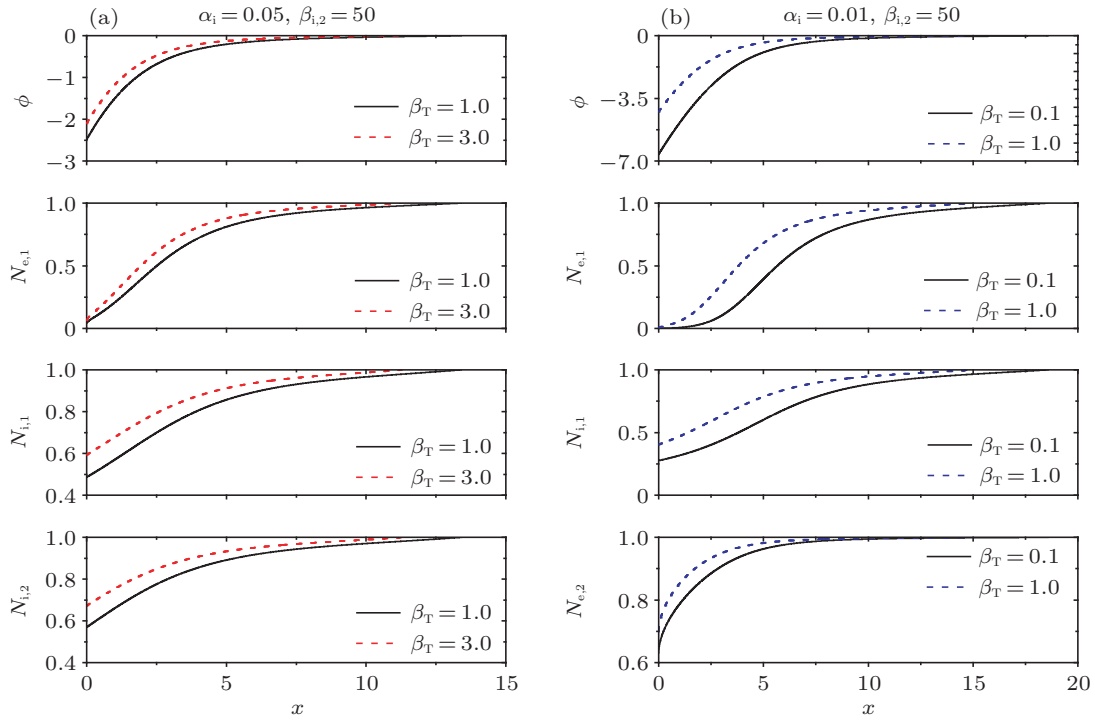



**Fig. 4.** (color online) Profiles of the normalized sheath potentials, background electron and ion densities, and energetic particle densities in the sheaths, with (a) energetic ion component and (b) energetic electron component, as a function of distance from the plasma sheath to the wall.

## 3. Dust particle in sheath

### 3.1. Dust charging in sheath

The dust particle begins to be charged by the collection of plasma and electron emission, when it meets the plasma. Usually, for a micron-sized charged grain, the dust charging time is much smaller than the characteristic time of the dust motion,[19,23] and then the equilibrium dust charge is related to the dust surface potential

$$Q_d = 4\pi\varepsilon_0 R_d \phi_d (1 + R_d/\lambda_{screen}), \tag{21}$$

where $R_d$ is the dust particle radius, $\phi_d$ is the dust surface potential, and $\lambda_{screen}$ is the screening length near the dust grain. Here, by following the method in Ref. [14], $\lambda_{screen} = \lambda_{lin}$ is used when $R_d > \lambda_{lin}$, where $1/\lambda_{lin}^2 = 1/\lambda_{De}^2 + 1/\lambda_{Di}^2$. While $R_d < \lambda_{lin}$, $\lambda_{screen} = \lambda_{De}$ is assumed. The dust surface potential is determined by a zero net current onto the dust particle, i.e.,

$$I_{i,j} + I_{e,j} + I_{es,j} = 0, \tag{22}$$

where the dust charging currents of the thermal plasma, energetic particle and emission electron are calculated in the framework of the orbital motion limited (OML) theory. We assume that the dust temperature is low and thermal radiation causes the dust particles to sufficiently cool so that the thermionic electron emission and mass sublimation/evaporation may not be taken into account.

In Eq. (22), the ion collection currents are[14]

$$I_{i,j} = e\pi R_d^2 n_{i,j} \sqrt{\frac{8k_B T_{i,j}}{\pi m_{i,j}}} \left[ \frac{\sqrt{\pi}}{4u} \left( 1 + 2u_j^2 - 2\frac{e\phi_d}{T_{i,j}} \right) \mathrm{erf}(u_j) + \frac{1}{2}\exp(-u_j^2) \right], \quad \phi_d < 0,$$

and

$$\begin{aligned} I_{i,j} = {} & e\pi R_d^2 n_{i,j} \sqrt{\frac{8k_B T_{i,j}}{\pi m_{i,j}}} \left[ \frac{\sqrt{\pi}}{8u}(1 + 2u_j^2 - 2u_m^2)(erf(u_j - u_m) \right. \\ & + \mathrm{erf}(u_j + u_m)) + \frac{1}{4}\left(1 + \frac{u_m}{u}\right)\exp(-(u_j - u_m)^2) \\ & \left. + \frac{1}{4}\left(1 - \frac{u_m}{u}\right)\exp(-(u_j + u_m)^2) \right], \quad \phi_d > 0, \end{aligned} \tag{23}$$

where $u_j = v_{i,j}/v_{thi}$ and $u_m = \sqrt{e\phi_d/k_B T_{i,j}}$, $\phi_d > 0$.

The thermal and energetic electron collection currents are

$$\begin{aligned} I_{e,j} &= (1 - \delta_{e,j}) e\pi R_d^2 n_{e,j} \sqrt{\frac{8k_B T_{e,j}}{\pi m_e}} \exp\left(\frac{e\phi_d}{k_B T_{e,j}}\right), \quad \phi_d < 0, \\ I_{e,j} &= (1 - \delta_{e,j}) e\pi R_d^2 n_{e,j} \sqrt{\frac{8k_B T_{e,j}}{\pi m_e}} \left(1 + \frac{e\phi_d}{k_B T_{e,j}}\right), \quad \phi_d > 0. \end{aligned} \tag{24}$$

The secondary emission current due to electron impact is given by[14]

$$\begin{aligned} I_{es,j} &= e8(\pi R_d/m_e)^2 \int_0^\infty E_p \delta(E) f_{es,j}(E_p - e\phi_d)\,\mathrm{d}E_p, \quad \phi_d < 0, \\ I_{es,j} &= e8(\pi R_d/m_e)^2 \exp\left(-\frac{e\phi_d}{k_B T_{es}}\right)\left(1 + \frac{e\phi_d}{k_B T_{es}}\right) \\ &\quad \times \int_{e\phi_d}^\infty E_p \delta(E) f_{es,j}(E_p - e\phi_d)\,\mathrm{d}E_p, \quad \phi_d > 0, \end{aligned} \tag{25}$$

with

$$f_{\mathrm{es},j}(E_\mathrm{p}-e\phi_\mathrm{d}) = n_{\mathrm{e},j}\left(\frac{m_\mathrm{e}}{2\pi T_{\mathrm{e},j}}\right)^{3/2}\exp\left(-\frac{E_\mathrm{p}-e\phi_\mathrm{d}}{k_\mathrm{B}T_{\mathrm{e},j}}\right)$$

and $T_\mathrm{es}$ being the temperature of the secondary emitted electron. Here, $T_\mathrm{es} = 1$ eV is used in the calculation.

Before presenting the numerical results of dust charging, it is worthwhile examining the applicability of the OML theory. The OML theory can be used to calculate dust charging currents if the condition $R_d << \lambda_\mathrm{De}$ is satisfied.[17,19] This implies that the dust particle radius $R_\mathrm{d}$ should be less than Debye length $\lambda_\mathrm{De}$; otherwise, there is no space for the dust particle to move from infinity to the grain surface, which is used for calculating the cross sections. However, in recent work,[32] it has been shown that there is very good agreement between OML theory and simulations until at least $R_\mathrm{d}/\lambda_\mathrm{De} = 5$. With the above sheath model parameters, we have $\lambda_\mathrm{De} \approx 7.0\times10^{-5}$ m. On the other hand, as mentioned in Section 1, the study in this paper is motivated due to the fact that the micron-sized charged grains can be utilized as a probe to study the sheath characteristics experimentally. In the present work, the maximum value of $R_\mathrm{d}$ is examined to be smaller than 20 μm, i.e., $R_\mathrm{d} < 20$ μm and then $R_\mathrm{d}/\lambda_\mathrm{De} < 0.3$. Therefore, our default parameters satisfy the condition $R_\mathrm{d}/\lambda_\mathrm{De} < 5$.

Making use of Eqs. (16)–(20), we can obtain numerically the local electric field, the ion density and velocity, and the electron density in the sheath, and then can calculate the dust surface potential in the sheath by using Eq. (22). Figures 5(a) and 5(b) show the spatial profiles of the normalized dust surface potential in the sheath for different energetic ion concentrations and energies, respectively. The dust charging caused by the energetic ion is higher (but not much higher) than by no energetic ion in the sheath because energetic ions do not play an important part in the charging process of dust in the range of our calculation parameters. With the increase of energetic ion concentration or energy, the dust surface potential becomes higher due to the larger ion flux following into the dust. For the same calculation parameters as shown in Fig. 5(c), the dust charges are higher in the case of a hydrogen ion as the energetic ion component than in the case of a deuterium ion as the energetic ion component. As seen from Fig. 2, either the hydrogen ion or deuterium ion is the energetic ion component, the profiles of the sheath potential and plasma variables are almost the same in the sheath, except that hydrogen energetic ion density is larger. Therefore, in the case of hydrogen ion as the energetic ion component, the larger energetic ion flux causes the higher dust surface potential. When the ratio of the thermal ion temperature to the electron temperature is changed, it is shown in Fig. 5(d) that the dust charge increases monotonically with increasing the temperature of the thermal background ion because ion flux increases.

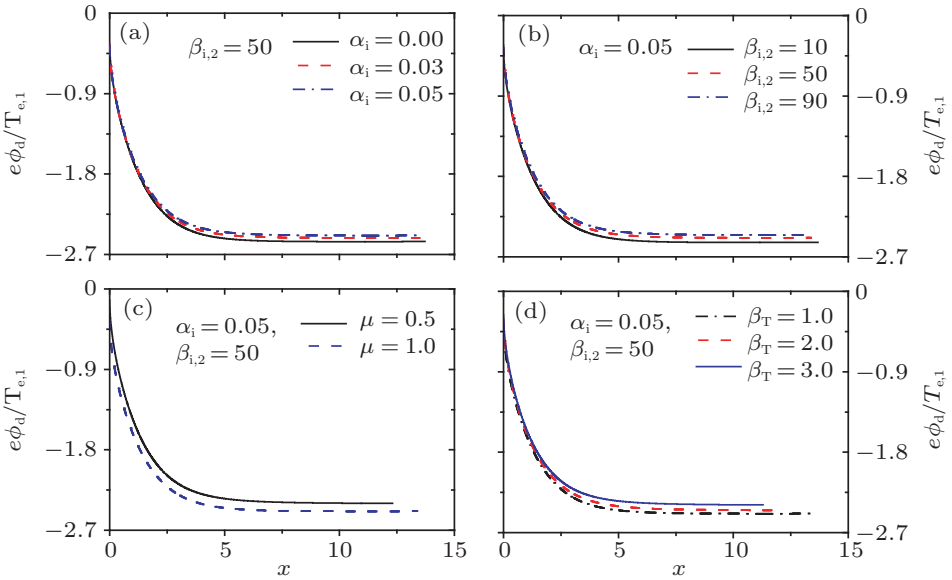



**Fig. 5.** (color online) Spatial profiles of the normalized dust surface potentials in the sheaths with (a) different energetic ion concentrations, (b) different energetic ion energies, (c) hydrogen ion and deuterium ion as energetic ion components, and (d) different ratios of the thermal ion temperature and electron temperature, respectively.

According to Fig. 3, the profiles of the sheath potential and plasma variables in the sheath depend strongly on the energetic electron, which indicate that the dust surface potential is a function of energetic electron. When an energetic electron component is present, we compare the spatial profiles of the normalized dust surface potential in the sheaths. As seen in Fig. 6, we can see a large negative dust surface potential near the wall in each of the cases where the energetic electrons have a large concentration or energy. This is due to the fact that at higher energetic electron concentration or energy, the sheath is dominated by the energetic electron, and then there are almost no thermal electrons near the wall. As a result, the zero net current flowing onto the dust surface requires the small energetic electron current. From Fig. 6, it is indicated that we

can discuss the sheath properties once obtaining the information about the dust charging since the energetic electron with a small concentration or energy can change significantly the dust surface potential in the charging process of dust.

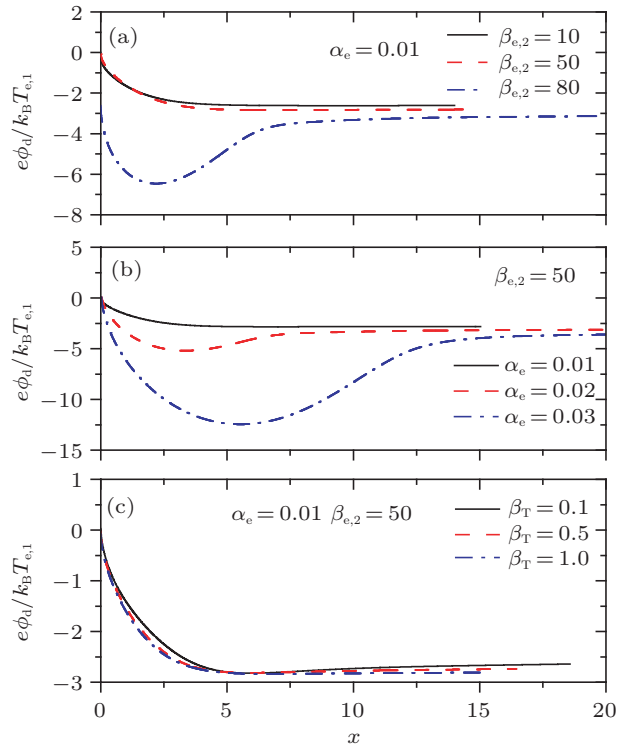



**Fig. 6.** (color online) Spatial profiles of the normalized dust surface potentials in the sheaths with (a) different energetic electron energies, (b) different energetic electron concentrations, and (c) different ratios of thermal ion temperature and electron temperature, respectively.

The effect of the background ion temperature on normalized dust surface potential is also shown in Fig. 6(c). We can see that the dust surface potential decreases with the increase of thermal ion temperature. The higher the thermal ion temperature, the lower the sheath potential will be since the thermal electron flux and energetic electron flux become larger. As a result, the repulsion of the less negatively charged wall allows the collection of less positive ions closer to the wall.

### 3.2. Levitating of dust in the sheath

The dynamics of dust in a plasma sheath has been investigated recently.[15,19,20] The dust can levitate in the sheath if it satisfies the force balance. Under this condition, the dust particle is stationary in the sheath and then the fine dust probe can provide the information about the sheath potential and sheath electric field, and about the plasma flux. Here, any moving dust particle is not considered since it is difficult to provide the sheath information.

To discuss the levitating of a dust particle in the sheath, we consider the total resultant force acting on the dust particle, which consists of gravitational force, electric force, and ion drag force, and is expressed as follows:

$$F_{\text{total}} = F_{\text{e}} + F_{\text{mg}} + F_{\text{id},j}. \tag{26}$$

The electric force in the sheath is

$$F_{\text{e}} = Q_{\text{d}} E. \tag{27}$$

The gravitational force can be expressed as

$$F_{\text{mg}} = m_{\text{d}} g = \frac{4\pi}{3} R_{\text{d}}^3 \rho_{\text{d}} g, \tag{28}$$

where $\rho_{\text{d}}$ and $g$ are the mass density of dust particle and acceleration of gravity, respectively. For the carbon dust particle$\rho_{\text{d}} = 2.25 \times 10^3$ kg·m$^{-3}$.

The ion drag force is normally made up of the contribution to the drag by the ions that are directly collected by the dust grain (denoted as $F_{\text{id,coll}}$) and the scattering part due to the Coulomb interaction between the dust grains and the ions (not collected by the grain) orbiting in the dust grain sheath (denoted as $F_{\text{id,orb}}$). For a negatively charged grain, the drag collection is given by[14]

$$\begin{aligned} & F_{\text{id,coll},j} \\ &= \pi R_{\text{d}}^2 m_{\text{i},j} n_{\text{i},j} v_{\text{thi},j} \left[ \frac{2}{\sqrt{\pi}} \left( \frac{1}{2} + u_j^2 - \frac{e\varphi_{\text{d}}}{k_{\text{B}} T_{\text{i},j}} \right) \exp(-u_j^2) \right. \\ &+ 2u_j \left( \frac{1}{2} + u_j^2 - \frac{e\varphi_{\text{d}}}{k_{\text{B}} T_{\text{i},j}} - \frac{1/2 - u_j^2 - e\varphi_{\text{d}}/k_{\text{B}} T_{\text{i},j}}{2u_j^2} \right) \\ &\left. \times \operatorname{erf}(u_j) \right] \frac{v_{\text{i},j}}{2u_j^2}, \end{aligned} \tag{29}$$

and for a positively charged grain[14]

$$\begin{aligned} F_{\text{id,coll},j} \;=\; & \pi R_{\text{d}}^2 m_{\text{i},j} n_{\text{i},j} v_{\text{thi}} \left\{ \frac{1}{\sqrt{\pi}} \left[ \left( 1 + 2u_j^2 + \frac{1 - 2u_j^2}{u_j} u_{\text{m},j} \right) \right. \right. \\ & \times \exp(-(u_j + u_{\text{m}})^2) + \left( 1 + 2u_j^2 - \frac{1 - 2u_j^2}{u_j} u_{\text{m},j} \right) \\ & \times \exp(-(u_j - u_{\text{m}})^2) + u_j (1 + 2(u_j^2 - e\varphi_{\text{d}}/k_{\text{B}} T_{\text{i},j}) \\ & - \frac{1 - 2(u_j^2 + e\varphi_{\text{d}}/k_{\text{B}} T_{\text{i},j})}{2u_j^2}) [\operatorname{erf}(u_j + u_{\text{m}}) \\ & \left. \left. + \operatorname{erf}(u_j - u_{\text{m}})] \right\} \frac{v_{\text{i},j}}{4u_j^2}. \end{aligned} \tag{30}$$

For the orbital part of the ion drag force,[14]

$$F_{\text{id,orb},j} = 2\pi R_{\text{d}}^2 m_{\text{i},j} n_{\text{i},j} v_{\text{thi}} v_j \left( \frac{e\phi_{\text{d}}}{k_{\text{B}} T_{\text{i},j}} \right)^2 \frac{C(u_j)}{u_j} \log \Lambda, \tag{31}$$

where

$$C(u_j) = \frac{1}{2u_j^2} \left[ \operatorname{erf}(u_j) - \frac{2u_j}{\sqrt{\pi}} \exp(-u_j^2) \right]$$

is the Chandrasekhar function, and

$$\log \Lambda = \frac{1}{2} \log \frac{b_{90}^2 + \eta_{\text{fit}}^2 \lambda_{\text{s}}^2}{b_{90}^2 + R_{\text{d}}^2}$$

is the Coulomb logarithm, from which the scattering$\Lambda$ is calculated, for a negatively charged grain with the impact parameter

$$b_{90,j} = -\frac{R_\mathrm{d}}{3+2u_j^2}\frac{e\phi_\mathrm{d}}{k_\mathrm{B}T_{\mathrm{i},j}},\quad \lambda_{\mathrm{s},j} = \lambda_\mathrm{De}\Big/\sqrt{1+\frac{3T_{\mathrm{e},1}}{T_{\mathrm{i},j}(3+2u_j^2)}}$$

is the screening length, and

$$\eta_{\mathrm{fit},j} = 1+\frac{R_\mathrm{d}}{\lambda_\mathrm{s}}\left(1+\sqrt{\frac{T_{\mathrm{e},1}}{6T_{\mathrm{i},j}}}\right).$$

For a positively charge grain, the Coulomb logarithm is given by

$$\begin{aligned}\log\Lambda \;=\; &\int_0^\infty \exp(-x)\log\left(1+4\left(\frac{\lambda_\mathrm{lin}k_\mathrm{B}T_{\mathrm{i},j}}{R_\mathrm{d}e\varphi_\mathrm{d}}\right)^2 x\right)\mathrm{d}x\\ &-2\int_{e\varphi_\mathrm{d}/k_\mathrm{B}T_{\mathrm{i},j}}^\infty \exp(-x)\log\left(\frac{2k_\mathrm{B}T_{\mathrm{i},j}}{e\varphi_\mathrm{d}}x-1\right)\mathrm{d}x.\end{aligned}$$

Before discussing the levitating of dust particle inside the sheath, we consider where it happens that electric force balances ion drag force and gravity. Figure 7(a) shows the profiles of electric force, ion drag force and gravity on a dust particle with $R_\mathrm{d} = 1$ μm. We can see that the electric force and ion drag force are the dominant force in the sheath. In a sheath of fusion plasma, the gravity is negligible unless the radius of dust grain $R_\mathrm{d} > 100$ μm.[14] The profile of total force which is the sum of electric force, ion drag force and gravity is also shown in Fig. 7(a). It is found that there are two balancing points corresponding to $F_\mathrm{total} = 0$. Whether the balancing point for the dust is stable is determined by the trapping potential energy. The dust particle trapping potential energy relative to the sheath edge with the dust particle trapping is $U_z(z) = -\int_0^Z F_\mathrm{total}(z')\,\mathrm{d}z'$ where $z = D - x$. From Fig. 7(b), we can see that the positions of $F_\mathrm{total} = 0$ are the peak and valley of the dust particle trapping potential energy and the stable position is only the valley of the dust particle trapping potential. Therefore, based on the forces balance, we can obtain the levitating position of the dust particle inside the sheath by analyzing the trapping potential energy.

First, we study the effect of the energetic ions on the stationary dust particle inside the sheath. Figure 8 shows the plots of levitation positions of the dust particles versus radius when the energetic ion component is present. With the increase of energetic ion concentration or energy, the radius of each of the dust particles levitating in the sheath decreases, and its levitating position is much closer to the wall. This is due to the fact that the effect of energetic ion on the dust charging causes the dust surface potential to become less negative and the electric force on dust is always negative in the whole sheath. Moreover, $F_\mathrm{e} \propto R_\mathrm{d}$ and $F_\mathrm{id} \propto R_\mathrm{d}^2$.

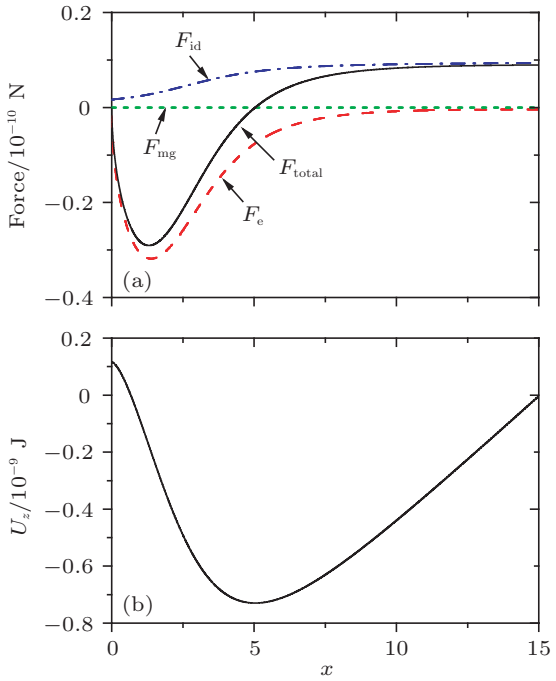



**Fig. 7.** (color online) (a) Forces and (b) trapping potential energy profiles as a function of distance from the sheath to the wall.

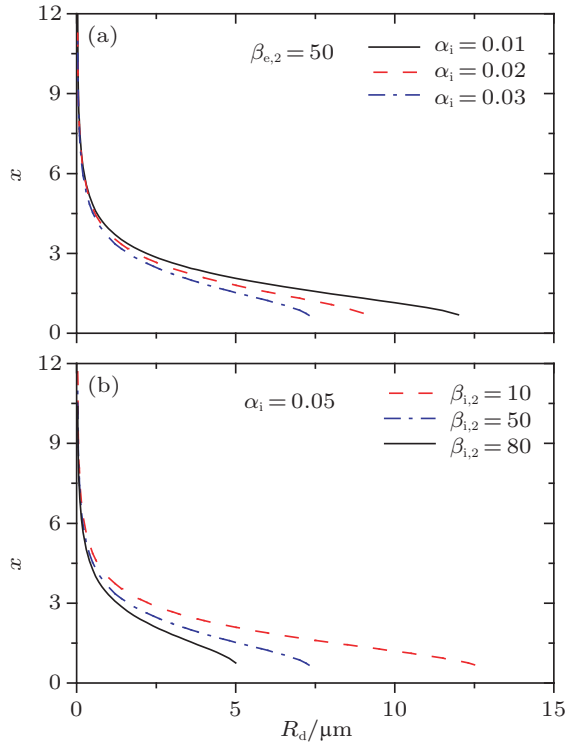



**Fig. 8.** (color online) Plots of levitation position versus radius of the carbon dust particle for (a) three different values of the energetic ion concentration, and (b) three different values of the energetic ion energy, respectively.

Next, we compare the levitating positions of dust particle inside the sheath in two cases of hydrogen ion and deuterium ion as energetic ions. From Fig. 9 it shows that the levitating position of the dust is much closer to the wall and the bigger dust particle can be trapped by the sheath in the case of deuterium ion as energetic ion. For the sheath of deuterium energetic ions, the dust particle feels the larger electric

force since it has more negative dust surface potential (seen in Fig. 5(c)). Meanwhile the ion drag force is also larger due to the deuterium ion mass being larger than the hydrogen ion mass. However, with increasing the radius of the dust particle, the ion drag force ($F_{\rm id} \propto R_{\rm d}^2$) increases faster than the electric force ($F_{\rm e} \propto R_{\rm d}$). As a result, with increasing the radius of dust, the difference between levitating positions of dust in two cases decreases and the bigger dust particle can be trapped by the sheath in the case of a deuterium ion as the energetic ion than in the case of a hydrogen ion as an energetic ion.

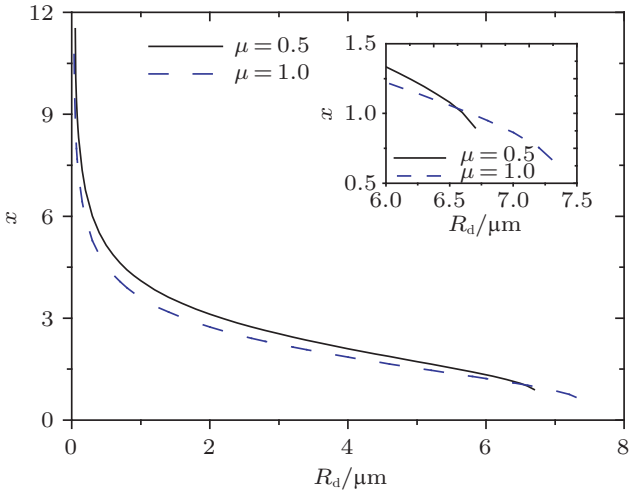



**Fig. 9.** (color online) Plots of the levitation position versus radius of carbon dust particle inside the sheath for the carbon wall in two cases of hydrogen ion and deuterium ion as energetic ions with $\alpha_{\rm i} = 0.05$ and $\beta_{i,2} = 50$.

Now, we investigate the effect of the energetic electron on the stationary dust particle inside the sheath. The levitating positions of the dust particles with different radii are shown in Fig. 10 for the different concentrations and energies of the energetic electrons. We can see that the levitating position of dust particle depends strongly on the energetic electron concentration or energy. Once the energetic electron dominates the sheath, the drop of sheath potential becomes very large and the dust surface potential near the wall region becomes very negative as shown in Figs. 6(a) and 6(b). Therefore, the deep well of the trapping potential energy is formed due to the large electric field force. As a result, the large radius dust particle can levitate inside the sheath and variation of its levitating position is small for $R_{\rm d} < 20$ μm. When the energetic electron concentration or energy increases, the levitating position is away from the wall due to the variation of electric force.

Finally, we investigate the effects of the background thermal ion temperature on the levitating position of dust inside the sheath of plasma containing energetic particles. We show the plots of the levitation position of dust particle versus dust radius for energetic ion with different ratios of thermal ion temperature to electron temperature in Fig. 11(a). For the same size dust particles, with the increase of the thermal ion temperature, their levitating position moves toward the wall, and

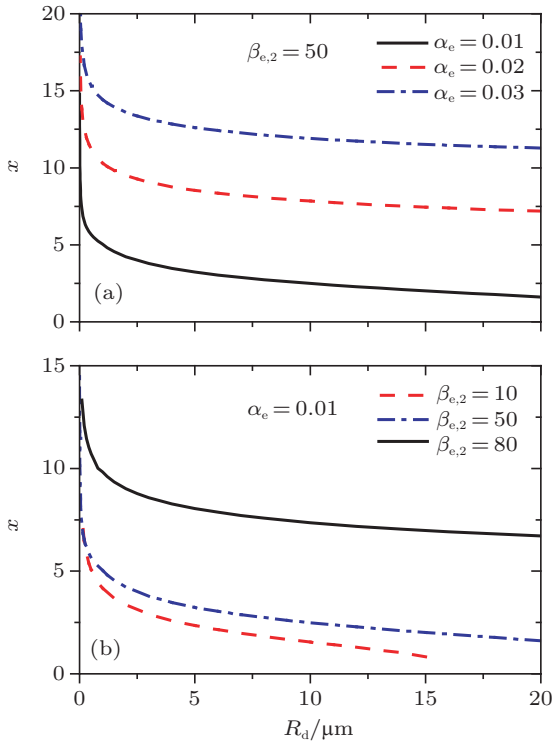



**Fig. 10.** (color online) Plots of levitation position versus balancing dust radius in the sheaths with (a) different energetic electron concentration and (b) different energetic electron energy, respectively.

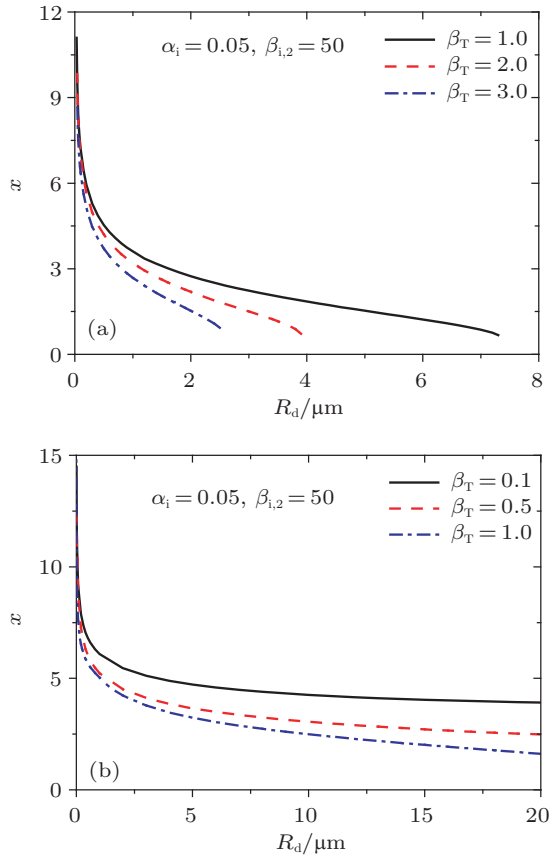



**Fig. 11.** (color online) Plots of levitation position versus balancing dust radius in the sheath for three different ratios of the thermal ion temperature to electron temperature.

the radius of the dust particle levitating inside the sheath decreases. The reason is that the less negative dust charges cause

the less negative electric force acting on the dust while the ion drag force increases with the increase of background thermal ion temperature. Figure 11(b) shows the plots of levitating position against dust radius in the sheath for energetic electron with different ratios of the thermal ion temperature and electron temperature. We can see that with the increase of thermal ion temperature, the levitating position moves toward the wall for the same size dust particles, and the larger size dust particle cannot stay in levitation equilibrium for the case of higher thermal ion temperature. The reason is that the ion drag force increases with the increase of background thermal ion temperature, while the electric force acting on the dust is less negative due to the smaller electric field as indicated in Fig. 4, although the dust surface potential is less negative as shown in Fig. 6(c).

## 4. Summary and conclusions

Using numerical simulations of the multi-fluid equations, we study the dynamics of a plasma sheath in the presence of energetic ions or energetic electrons. It is found that the sheath potential depends on both energetic particle concentration and energy. By comparing two cases of the hydrogen ion and deuterium ion as the energetic ion component, the results show that the profiles of the sheath potential and plasma variables including thermal background densities of ion and electron are almost the same in the sheath, except that hydrogen energetic ion density is larger. The pronounced effect of the energetic electron is present for the carbon wall even for a small fraction of energetic electron concentration or energy. In addition, the influence of the ratio of the thermal background ion temperature to electron temperature on the sheath structure is also examined.

Based on the OML theory, a dust grain charging in the sheath of plasma containing energetic particles is investigated. The dust surface potential decreases with increasing energetic ion concentration or energy, while it increases with increasing thermal background ion temperature. In the case of a hydrogen ion as the energetic ion component, the dust acquires less negative charges than in the case of a deuterium ion as the energetic ion component. When the energetic electron component is present, it changes the dust surface potential. A large negative dust surface potential near the wall is observed when the energetic electron concentration or energy exceeds a certain value. The reason is that there are almost no thermal electrons near the wall and the energetic electron from the plasma region plays an important part in the charging process of dust. Even if the energetic ion or electron component is present, the dust surface potential decreases with the increase of thermal background ion temperature.

By analyzing the trapping potential energy, we can obtain the stable point of dust whose total resultant force is zero in the sheath. When the energetic ion concentration or energy increases, the radius of dust particle trapped by the sheath decreases and the levitating position is much closer to the wall. The difference in the levitating position of the dust particle inside the sheath between the cases of hydrogen ion and deuterium ion as energetic ions decreases, and the bigger dust particle can be trapped by the sheath in the case of deuterium ion as energetic ions. By investigating the effect of the energetic electron on the stationary dust particle inside the sheath, it is found that the levitating positions of the dust particles with different sizes depend strongly on the energetic electron concentration and energy. Once the energetic electron dominates the sheath, the large radius dust particle can levitate inside the sheath and variation of their levitating position is small for $R_d < 20$ μm because of the deep well of the trapping potential energy near the wall is formed due to the large electric field force. With the increase of energetic electron concentration or energy, the levitating position of the dust particle is away from the wall. As the thermal background ion temperature increases, for the cases of sheath plasma containing energetic ions and energetic electrons, respectively, the levitating position of the dust particle inside the sheath moves toward the wall for the same size dust particles, and the larger size dust particle cannot stay in levitation equilibrium for the higher background ion temperature.

Our results presented in this work are of importance for plasma diagnostic when the energetic particle component is present in plasma since the plasma-wall interaction can be studied in considerable detail by using fine dust probes, which will provide, though indirectly, a useful guide in measuring the sheath characteristics because the charge on the grain is a function of the local plasma condition. Finally, note that our sheath model and calculation of dust charging rely on several assumptions for the sake of simplicity. For example, magnetic field is not taken into account. For a magnetized sheath, the sheath structure depends strongly on the magnitude and direction of the magnetic field,[33] and the dust particle charging process is modified by the magnetic field.[34] In future work, we will investigate dust levitating in the magnetized sheath when the energetic electron component is present.

## References


[1] Heidbrink W W and Sadler G J 1994 *Nucl. Fusion* **34** 535
[2] Basiuk V, Eriksson L G, Bergeaud V, Chantant M, Martin G, Nguyen F, Reichle R, Vallet J C, Delpeche L and Surle F 2004 *Nucl. Fusion* **44** 181
[3] Zhu Y B, Heidbrink W W and Pickering L D 2010 *Nucl. Fusion* **50** 084024
[4] Li Y L, Xu G S, Wang H Q, Xiao C, Wan B N, Gao Z, Chen R, Wang L, Gan K F, Yang J H, Zhang X J, Liu S C, Li M H, Ding S, Yan S N, Zhang W, Hu G H, Liu Y L, Shao L M, Li J, Chen L, Zhao N, Xu J C, Yang Q Q, Lan H and Ye Y 2015 *Phys. Plasmas* **22** 022510
[5] Wu B, Hao B, White R, Wang J, Zang Q, Han X and Hu C 2017 *Plasma Phys. Control. Fusion* **59** 025004
[6] Tang T, Hu J S, Li J G, Li Y Y, Morfill G and Ashikawa N 2011 *J. Nucl. Mater.* **415** S1094

[7] West W P and Bray B D 2007 *J. Nucl. Mater.* **363–365** 107
[8] Shiraishi K and Takamura S 1992 *Contrib. Plasma Phys.* **32** 243
[9] Stangeby P C 1995 *Plasma Phys. Control. Fusion* **37** 1031
[10] Tskhakaya D, Kuhn S, Petrzilka V and Khanal R 2002 *Phys. Plasmas* **9** 2486
[11] Ou J, Lin B B, Zhao X Y and Yang Y L 2016 *Plasma Phys. Control. Fusion* **58** 075004
[12] Ou J, Xiang N, Gan C Y and Yang J H 2013 *Phys. Plasmas* **20** 063502
[13] Lin B B, Xiang N, Ou J and Zhao X Y 2017 *Chin. Phys. Lett.* **34** 5203
[14] Delzanno G L and Tang X 2014 *Phys. Plasma* **21** 022502
[15] Pandey B P, Samarian A and Vladimirov S V 2007 *Phys. Plasma* **14** 093703
[16] Beadles R, Wang X and Horanyi M 2017 *Phys. Plasma* **24** 023701
[17] Foroutan G and Akhoundi A 2012 *Phys. Plasmas* **19** 103505
[18] Chung T H 2014 *J. Korean Phys. Soc.* **65** 1873
[19] Nitter T 1996 *Plasma Sources Sci. Technol.* **5** 93
[20] Wang D, Liu D and Liu J 2000 *J. Appl. Phys.* **88** 1276
[21] Wu J, Liu G, Y L M and Duan R X 2012 *Acta Phys. Sin.* **61** 075205 (in Chinese)
[22] Zou X 2006 *Chin. Phys. Lett.* **23** 396
[23] Liu J Y, Chen L ,Wang F, Wang N and Duan P 2010 *Acta Phys. Sin.* **59** 8692 (in Chinese)
[24] Kawamura G, Tomita Y and Kirschner A 2013 *J. Nucl. Mater.* **438** S909
[25] Sun Z Y, Sang C F, Hu W P and Wang D Z 2014 *Acta Phys. Sin.* **63** 145204 (in Chinese)
[26] Stangeby P C 2000 *The Plasma Boundary of Magnetic Fusion Devices* (Bristol: IOP Publishing)
[27] Young J R 1957 *J. Appl. Phys.* **28** 524
[28] Walker C G H, El Gomati M M, Assa'd A M D and Zadrazil M 2008 *Scanning* **30** 365
[29] Franklin R N 2003 *J. Phys. D: Appl. Phys.* **36** 1806
[30] Cercek M, Filipic G, Gyergyek T and Kovacic J 2010 *Contrib. Plasma Phys.* **50** 909
[31] Riemann K U 1995 *IEEE Trans. Plasma Sci.* **23** 4
[32] Delzanno G L and Tang X 2015 *Phys. Plasmas* **22** 113703
[33] Zou, X, Liu J Y, Wang Z X, Gong Y, Liu Y and Wang X G 2004 *Acta Phys. Sin.* **53** 3409 (in Chinese)
[34] Salimullah M, Sandberg I and Shukla P K 2003 *Phys. Rev. E* **68** 027403